Available online at www.sciencedirect.com
ScienceDirect
Journal of Hazardous Materials 150 (2008) 626–641
Journal of Hazardous Materials
www.elsevier.com/locate/jhazmat

Liquid-phase adsorption of phenols using activated carbons derived from agricultural waste material

Kunwar P. Singh [a,*], Amrita Malik [a], Sarita Sinha [b], Priyanka Ojha [a]

[a] *Environmental Chemistry Section, Industrial Toxicology Research Centre, Post Box 80, MG Marg, Lucknow 226001, India*
[b] *National Botanical Research Institute, Rana Pratap Marg, Lucknow 226001, India*

Received 12 August 2005; received in revised form 7 March 2007; accepted 8 May 2007
Available online 22 May 2007

Abstract

Physical and chemical properties of activated carbons prepared from coconut shells (SAC and ATSAC) were studied. The adsorption equilibria and kinetics of phenol and 2,4-dichlorophenol from aqueous solutions on such carbons were then examined at three different temperatures (10, 25 and 40 °C). Adsorption of both phenol and 2,4-dichlorophenol increased with an increase in temperature. The experimental data were analyzed using the Langmuir and Freundlich isotherm models. Both the isotherm models adequately fit the adsorption data for both the phenols. The carbon developed through the acid treatment of coconut shells (ATSAC) exhibited relatively higher monolayer adsorption capacity for phenol (0.53 mmol g^{-1}) and 2,4-dichlorophenol (0.31 mmol g^{-1}) as compared to that developed by thermal activation (SAC) with adsorption capacity of 0.36 and 0.20 mmol g^{-1}, for phenol and 2,4-dichlorophenol, respectively. The equilibrium sorption and kinetics model parameters and thermodynamic functions were estimated and discussed. The thermodynamic parameters (free energy, enthalpy and entropy changes) exhibited the feasibility and spontaneous nature of the adsorption process. The sorption kinetics was studied using the pseudo-first-order and second-order kinetics models. The adsorption kinetics data for both the phenol and 2,4-dichlorophenol fitted better to the second-order model. An attempt was also made to identify the rate-limiting step involved in the adsorption process. Results of mass transfer analysis suggested the endothermic nature of the reaction and change in the mechanism with time and initial concentration of the adsorbate. The results of the study show that the activated carbons derived from coconut shells can be used as potential adsorbent for phenols in water/wastewater.

Keywords: Adsorption; Equilibria; Kinetics; Phenols; Activated carbons; Coconut shell

1. Introduction

Discharge of wastewater/effluent containing organic pollutants into natural surface waters poses serious risk to aquatic organisms and human beings besides imparting a carbolic odor to the receiving water. Phenols find their way into surface water from industrial effluents such as those from coal tar, gasoline, plastic, rubber-proofing, disinfectant, pharmaceutical and steel industries, domestic wastewaters, agricultural runoff and chemical spillage [1]. Contamination of groundwater aquifers with phenolic compounds has been reported [2]. The health effects following repeated exposure to low levels of phenol in water include liver damage, diarrhea, mouth ulcers, dark urine and hemolytic anemia. In animals, spilling of dilute phenol solution on the portion greater than 25% of the body surface may result in death [3]. Phenols have been registered as priority pollutants by the US Environmental Protection Agency (USEPA) with a permissible limit of 0.1 mg L^{-1} in wastewater [4]. According to the Bureau of Indian Standards [5] (BIS), the permissible limit of phenol for drinking water is 1.0 μg L^{-1}.

The methods used for the treatment of water/wastewater containing phenolic wastes include microbial degradation [6], chemical oxidation [7], photocatalytic degradation using TiO_2 [8], sonophotochemical [9], ultrasonic degradation [10], enzymatic polymerization [11] and adsorption [12], etc. Among these, adsorption offers an efficient and economically feasible technology for the removal of contaminants from wastewa-

* Corresponding author. Tel.: +91 522 2508916; fax: +91 522 2628227.
E-mail addresses: kpsingh_52@yahoo.com, kunwarpsingh@gmail.com (K.P. Singh).

0304-3894/$ – see front matter © 2007 Elsevier B.V. All rights reserved.
doi:10.1016/j.jhazmat.2007.05.017

ters. Selective adsorption utilizing biological materials, mineral oxides, and activated carbon or polymer resins has developed great interest among the researchers and environmentalists. Activated carbon has been utilized as an efficient sorbent for odor removal, solvent recovery, decolorization, dechlorination, ozone annihilation, H_2S/CS_2 removal, gold recovery, filtration, condensed deviling, fuel gas cleaning, industrial wastewater treatment, drinking water conditioning, etc. Activated carbons can be prepared from a variety of materials. The most commonly used raw materials for the preparation of activated carbons in commercial practice are peat, coal, lignite, wood and agricultural by-products. Production of activated carbon from agricultural by-products serves a double purpose by converting unwanted, surplus agricultural waste to useful, valuable material and provides an efficient adsorbent material for the removal of organic pollutants from water/waste water.

Activated carbons have a large adsorption capacity for a variety of organic pollutants but are expensive due to difficult regeneration and higher disposal cost [12–18]. In view of the high cost and tedious procedure for the preparation and regeneration of activated carbon, there is continuing search for the development of adsorbents using cheaper raw materials. Many researchers have studied the feasibility of less expensive activated carbons prepared from spent oil shake [14], bagasse fly ash [1], tamarind nut [15], soyabean hulls [16], salvinea molta Mitchell [17], and coconut husk [18] for the removal of phenolic compounds.

For any sorbent to be feasible, it must combine high and fast adsorption capacity with inexpensive regeneration [12]. The present study is aimed towards the development of an industrially viable, cost effective and environmentally compatible adsorbent for the removal of phenol from wastewater. For this purpose, the coconut shells, which are by-product of coconut based industries, were converted into an inexpensive carbonaceous adsorbent. To evaluate the efficiency of developed adsorbents, adsorption batch and kinetic studies were performed.

2. Materials and methods

All reagents and chemicals used in the study were of AR grade. Stock solutions of the test reagents were prepared by dissolving the desired amount of phenol/2,4-dichlorophenol in double distilled water. pH of the test solution was adjusted using reagent grade dilute sulfuric acid and sodium hydroxide.

2.1. Adsorbent development and characterization

The raw material, i.e. coconut shells (agricultural waste materials) was collected from the local market of Lucknow City, India. The collected material was thoroughly washed with double distilled water to remove any extraneous depositions and dried at room temperature. Two types of carbonaceous material were prepared. First type of carbon was prepared by treating one part of coconut shells with two parts (by weight) of concentrated sulfuric acid and the same were kept in an oven maintained at 150–165 °C for a period of 24 h. The carbonized material was washed well with double distilled water to remove the free acid and dried at 105–110 °C for 24 h and subjected to thermal activation at different temperatures viz., 200, 400, 600 and 800 °C for 1 h in an inert atmosphere. Second type of carbon was prepared by activating the coconut shells without any chemical treatment at different temperatures viz., 200, 400, 600 and 800 °C for 1 h in an inert atmosphere. Activation is carried out under closely controlled process parameters to get optimum properties. Finally, the product is adequately cooled before it is exposed to the atmosphere. The temperature and time were optimized by observing the surface properties of the activated products obtained. In both the cases the products obtained at temperatures higher or lower than 600 °C exhibited less adsorption capacities. The products so obtained were sieved to the desired particle sizes, such as 30–200, 200–250 and 250–300 mesh. Finally, products were stored in a vacuum desiccator until required. The developed carbons were designated as SAC (activated carbon derived from coconut shells) and ATSAC (activated carbon derived from acid treated coconut shells).

The chemical and textural composition of the developed adsorbents was established by carrying out the proximate, elemental analysis by gas adsorption, mercury porosimetry, and helium & mercury density measurements, respectively. The values of the BET specific surface area (S_{BET}) and pore volumes (micropore volume, V_{mi}; mesopore volume, V_{me}; macropore volume, V_{ma}; and total pore volume, V_T) were determined using Quantachrome surface area analyzer model Autosorb-1. The mercury porosimetries have been carried out with a Quantachrome porosimeter model Autoscan-60. The mercury density was determined as usual, when carrying out the mercury porosimetery experiments. The helium density was measured using a Quantachrome Stereopycnometer. The chemical constituents of activated carbons were determined following the methods reported elsewhere [19,20]. SEM was used to investigate the surface topography of the activated carbon. Samples were set in epoxy and were placed in the sample chamber and evacuated to high vacuum (2×10^6 Torr). The sample is bombarded with a finely focused electron beam. A three-dimensional topographic image (SEM micrographs) is formed by collecting the secondary electrons generated by the primary beam.

The pH measurements were made using a pH meter (Model 744, Metrohm). Absorbance measurements were made on a GBC UV–visible spectrophotometer model Cintra-40. The spectrophotometer response time was 0.1 s and the instrument had a resolution of 0.1 nm. Absorbance values were recorded at the wavelength for maximum absorbance (λ_{max}), i.e. 269 and 284 nm for phenol and 2,4-dichlorophenol, respectively. The concentrations of respective compounds were measured with a 1-cm light-path cell, with an absorbance accuracy of ±0.004 at λ_{max}.

2.2. Sorption procedure

Sorption studies were performed by the batch technique to obtain rate and equilibrium data. The batch technique was used due to its simplicity. In order to select the optimum pH for adsorption experiments, a series of batch experiments with the

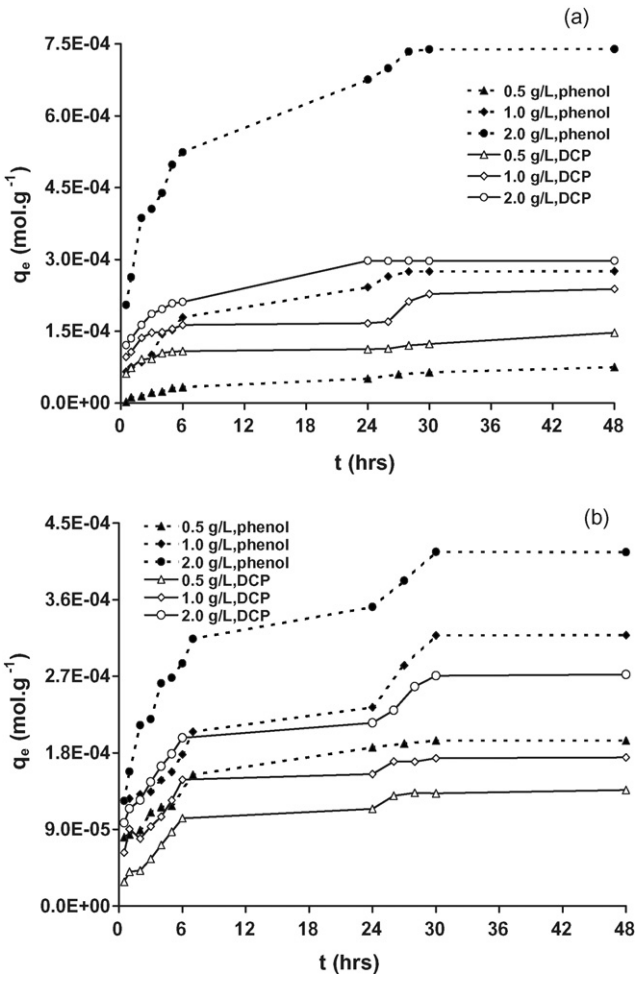

Fig. 1. Effect of adsorbent amount on the uptake of phenol and 2,4-dichlorophenol by (a) SAC and (b) ATSAC at optimum pH, temperature 25 °C; $C_0 = 5 \times 10^{-4}$ mol L^{-1}.

SAC and ATSAC were conducted at different pH ranging 2–10. Batch sorption studies were performed at different temperatures (10, 20 and 40 °C) and at optimum pH to obtain data on the rate and extent of sorption. For isotherm studies, a series of 100-mL Erlenmeyer stoppered conical flasks containing 50 mL of adsorbate (phenol or 2,4-dichlorophenol) solution of desired pH of varied concentrations (10^{-4} to 10^{-3} mol L^{-1}) and definite amount of adsorbents (30–200 mesh) were mixed together and agitated intermittently for a period of 30 h. The contact time and other conditions were selected on the basis of preliminary experiments, which demonstrated that the equilibrium was established in 28–30 h as can be seen from the results in Fig. 1a and b. Equilibrium for longer times, gave practically the same uptake, therefore the contact period was 30 h in all the equilibrium studies. After this period the solution was filtered and the phenol and 2,4-dichlorophenol concentrations were determined spectrophotometrically at the corresponding λ_{max}. The effect of adsorbent amount viz., SAC and ATSAC on the rate of uptake of adsorbate is shown in Fig. 1a and b, respectively. The uptake increases with an increase in the adsorbent amount. The amount of adsorbent has been kept 1.0 g L^{-1} in all the subsequent studies.

2.3. Kinetic studies

The adsorption kinetics of different adsorbates (phenol and 2,4-dichlorophenol) on the adsorbents (SAC and ATSAC) derived from coconut shells was studied by the batch technique. The batch kinetic studies were performed at different temperatures, adsorbate concentrations, and adsorbent doses at optimum pH. For this purpose, a number of stoppered conical flasks containing a definite volume (50 mL in each case) of adsorbate solution of known concentrations were placed in a thermostat controlled shaking assembly. When the desired temperature reached, a known amount of adsorbent was added to each flask and the solutions were agitated mechanically. At predecided intervals of time, the solutions of the specified conical flasks were separated from the adsorbent and analyzed spectrophotometrically to determine the uptake of adsorbate (phenol and 2,4-dichlorophenol) at corresponding λ_{max}.

2.4. Modeling

2.4.1. Equilibrium isotherm models

The Langmuir and Freundlich models [21] were used to fit the adsorption isotherms and to evaluate the isotherm parameters. The Langmuir isotherm is based upon the assumption of monolayer adsorption onto a surface containing finite number of adsorption sites of uniform energies of adsorption with no transmigration of adsorbate in the pores of the adsorbent surface. The Langmuir equation may be written as:

$$\frac{C_e}{q_e} = \frac{1}{Q^0 b} + \frac{1}{Q^0} C_e \quad (1)$$

where q_e is the amount of solute adsorbed per unit weight of adsorbent (mol g^{-1}), C_e the equilibrium concentration (mol L^{-1}), Q^0 the monolayer adsorption capacity (mol g^{-1}) and b is the constant related to the free energy of adsorption ($b \propto e^{-\Delta G/RT}$). It is the value reciprocal of the concentration of which half the saturation of the adsorbent is attained. The model parameters (Q^0 and b) can be determined from the linear plots of C_e/q_e and C_e.

The Freundlich model assumes heterogeneous surface energies, in which adsorption energy varies as a function of the surface coverage due to variation in the heat of adsorption. The Freundlich equation may be written as:

$$\log q_e = \log K_F + \frac{1}{n} \log C_e \quad (2)$$

where q_e is the amount of solute adsorbed per unit weight of adsorbent (mol g^{-1}), C_e the equilibrium concentration (mol L^{-1}), K_F the constant indicative of the relative adsorption capacity of the adsorbent (mol g^{-1}) and $1/n$ is the constant, indicative of the intensity of the adsorption. The model parameters (K_F and $1/n$) can be determined from the linear plots of log q_e and log C_e. The Freundlich model is widely applied [13,22,23] in heterogeneous systems especially of organic compounds and highly interactive species on activated carbon and molecular sieves.

2.4.2. Kinetic models

To analyze the adsorption rate of phenols onto the developed adsorbents, two kinetic models (pseudo-first-order and pseudo-second-order) were used.

The pseudo-first-order-kinetic equation [24] may be written as:

$$\log(q_e - q_t) = \log q_e - \frac{k_1}{2.303}t \quad (3)$$

where q_e and q_t are the amounts adsorbed at equilibrium and at time t, respectively, and k_1 is the first-order rate constant. The adsorption rate parameter k_1 can be calculated by plotting $\log(q_e - q_t)$ versus 't'.

The pseudo-second-order-equation based on equilibrium adsorption may be expressed as [25]:

$$\frac{t}{q_t} = \frac{1}{v_0} + \frac{1}{q_e}t \quad (4)$$

where $v_0(k_2 q_e^2)$ is the initial sorption rate, q_e the amount adsorbed at equilibrium, and k_2 is the pseudo-second-order rate constant. The values of k_2, v_0 and q_e can be calculated by plotting t/q_t versus 't'.

3. Results and discussion

3.1. Characterization

For characterization of the prepared activated carbons, 1.0 g of each was stirred with deionized water (100 mL, pH 6.8) for two hrs and left for 30 h in an air tight stoppered conical flask. After the equilibration time of 30 h, a rise in pH was observed in case of SAC, while there was lowering of pH in case of ATSAC. As a result, the SAC may be considered as H-type carbon in nature and ATSAC as L-type. H-type activated carbons assume a positive charge (protonated) upon introduction to water (yielding alkaline pH), are hydrophobic, and can adsorb strong acids. The predominant surface oxides on the surface of an H-type carbon are lactones, quinones, phenols and carboxylates [26]. L-type activated carbons assume a negative charge (ionised) upon hydration (yielding acidic pH), are hydrophilic, and can neutralise strong bases. The predominant surface functional groups for L-type carbons according to Garten and Weiss [27] are carboxyl, phenolic hydroxyl, carbonyl (quinone type), carboxylic acid, anhydrides, lactone and cyclic peroxide [28].

The specific surface area of the carbons was evaluated from the N_2 isotherms by applying the Brunaeur, Emmett and Teller (BET) equation at a relative pressure (p/p_0) of 0.35 and a_m equal to 16.2 Å (a_m is the average area covered by a molecule of N_2 in completed monolayer). From the aforesaid isotherms as well, the micropore volume (W_0) has been obtained by taking it to be equal to the volume of N_2 adsorbed at $p/p_0 = 0.10(V_{mi})$ and also by applying the Dubinin–Radushkevich equation.

The volumes of mesopores (V_{me}) and macropores (V_{ma}) have been derived from the curves of cumulative pore volume (V_{cu}) against pore radius (r) (mercury porosimetry): $V_{me} = V_{cu}$(at $r = 10$ Å) $- V_{ma}$ and $V_{ma} = V_{cu}$ (at $r = 250$ Å). The total pore volume has been calculated by adding up V_{mi}, V_{me} and V_{ma}.

Table 1
Characteristics of developed activated carbons (SAC and ATSAC)

Adsorbent	S_{BET} ($m^2\,g^{-1}$)	V_{mi} ($cm^3\,g^{-1}$)	W_o ($cm^3\,g^{-1}$)	V_{me} ($cm^3\,g^{-1}$)	V_{ma} ($cm^3\,g^{-1}$)	V_T ($cm^3\,g^{-1}$)	ρ_{Hg} ($g\,cm^3$)	ρ_{He} ($g\,cm^3$)	Ash (%)	C (%)	N (%)	H (%)	pH	Yield (%)
SAC	378	0.12	0.12	0.05	0.09	0.26	1.54	0.98	68.23	69.23	0.25	2.21	7.02	21.29
ATSAC	380	0.12	0.13	0.05	0.19	0.36	1.60	0.91	62.65	76.64	0.28	2.26	5.72	99.35

$V_{me} = V_{cu}$(at $r = 20$ Å) $- V_{ma}$, $V_{ma} = V_{cu}$ (at $r = 250$ Å), V_{cu} = cumulative pore volume (mercury porosimetry), $V_T = V_{mi} + V_{me} + V_{ma}$.

The different chemical constituents of activated carbons along with other characteristics are given in Table 1. It may be noted that ATSAC has relatively higher surface area and lower ash content than SAC. The ATSAC also showed higher pore volume (0.36 $cm^3\,g^{-1}$) and carbon content (76.64%) as compared to SAC (0.26 $cm^3\,g^{-1}$ and 69.23%, respectively). There was a large difference between the yield of ATSAC (about 99%) and SAC (about 21%). The difference between the two (SAC and ATSAC) may be attributed to the chemical treatment of the later. The chemical treatment results in a relatively larger yield as compared to the physical activation methods and good development of the porous structure [29]. The chemical treatment leads to the dehydration of cellulosic material during pyrolysis resulting into charring and aromatization of the carbon skeleton, and the creation of the porous structure [30]. Further, both the SAC and ATSAC prepared here have surface area, meso- and micropores comparable with other carbons derived from waste materials [31,32], these have relatively low surface area and pore volumes as compared to those available commercially [33–35]. SEM is widely used to study the morphological features and surface characteristics of the adsorbent materials. In the present study, scanning electron microscopic photograph (1000× magnification) of developed activated carbons (30–200 mesh) revealed surface texture, porosity and fibrous structure of the developed adsorbents (Fig. 2). The rough surface micrographs showed a distinct roughness with oval pattern. The identification of various forms of different constituents in activated carbon viz., SAC and ATSAC has been done with the help of IR spectra [36]. The IR spectrum of the activated carbons (Fig. 3a and b) showed weak and broad peaks in the region of 3853–453 cm^{-1}. Approximate FT-IR band assignment indicated the presence of carbonyl, carboxyls, lactones, phenols, olefinic and aromatic structures. The 1800–1540 cm^{-1} band is associated with C=O stretching mode in carbonyls, carboxylic acids, and lactones and C=C bonds in olefinic and aromatic structures, whereas the 1440–1000 cm^{-1} band was assigned to the C–O and O–H bending modes. Further, presence of relatively weak peak/band of the hydroxyl group (centered around 3400 cm^{-1}) differentiated between the two adsorbents. The assignment of a specific wave number to a given functional group was not possible because the absorption bands of various functional groups overlap and shift, depending on their molecular structure and environment. Shifts in absorption positions can be caused by the factors such as intramolecular and intermolecular hydrogen bonding, steric effects, and degrees of conjugation.

3.2. Sorption studies

The pH of the solution is one of the major factors influencing the adsorption capacity of compounds that can be ionized. Acid or alkali species may change the surface chemistry of the adsorbent by reacting with surface groups. These effects may lead to significant alterations in the adsorption equilibrium depending on the pH [37]. At higher pH the phenols dissociate, forming phenolate anions, whereas surface functional groups may be either neutral or negatively charged. The electrostatic repulsion between the like charges lowers the adsorption capacities in case

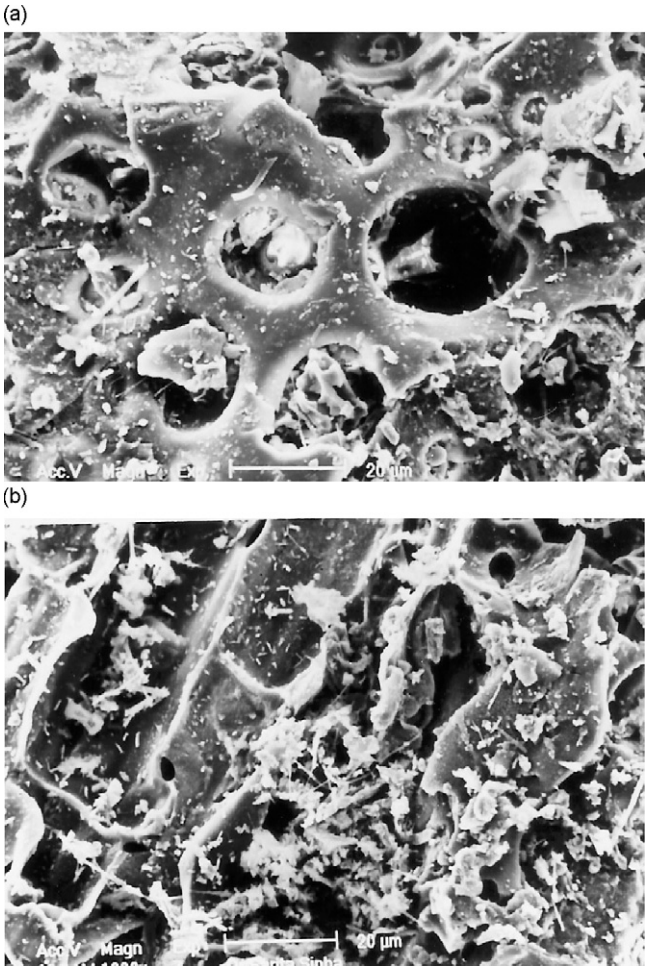

Fig. 2. Scanning electron micrographs (SEM) of (a) SAC and (b) ATSAC at 1000×.

of both the phenols [23]. This may be due to the dependence of phenol ionization on pH of the medium. The ionic fraction of phenolate ion, φ_{ions} can be calculated from the equation [38]:

$$\varphi_{ions} = \frac{1}{[1 + 10^{(pK_a - pH)}]} \quad (5)$$

The φ_{ions} increases as the pH value increased. Thus, phenols being weak acid ($pK_a = 9.89$ and 7.8 for phenol and 2,4-dichlorophenol, respectively) will be adsorbed to a lesser extent at higher pH values due to the repulsive force prevailing at higher pH [38,39]. Phenol and 2,4-dichlorophenol are associated with the electron withdrawing effect of the aromatic ring [23]. Adsorption capacity of the activated carbons for the solute in molecular form depends on the electron density of the solute and the carbon surface because the dispersive interaction between the aromatic ring of the solute and those of the carbon surface are the main forces involved in the adsorption process [40]. The effect of pH on the removal of different adsorbates (phenol and 2,4-dichlorophenol) using developed adsorbents (SAC and ATSAC) is presented in Fig. 4. These studies were carried out at the initial adsorbate concentration of 1×10^{-4} mol L^{-1}. It was observed that the removal decreases with an increase in the solution pH. The maximum adsorption was observed at the acidic pH for both

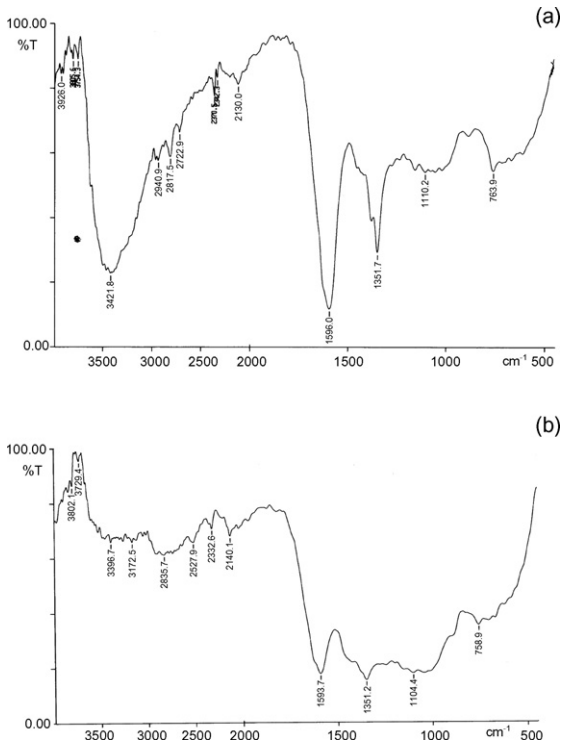

Fig. 3. IR spectrum of (a) ATSAC and (b) SAC.

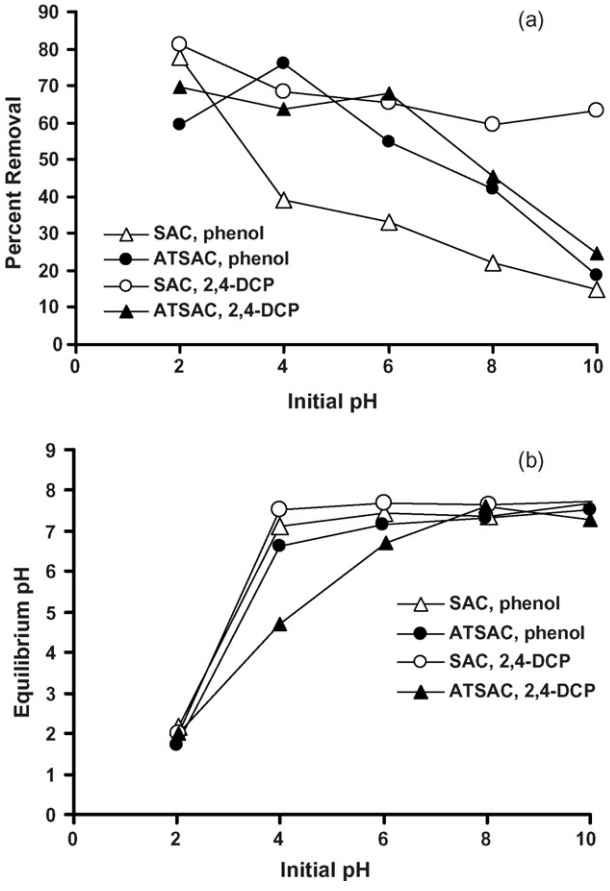

Fig. 4. Effect of pH on the (a) adsorption of phenol and 2,4-dichlorophenol and (b) equilibrium pH on SAC and ATSAC.

the adsorbents, therefore, a pH of 2.0 ± 0.2 was chosen for the adsorption of phenol on the SAC and 4.0 ± 0.2 for the adsorption on ATSAC (Fig. 4a). In case of 2,4-dichlorophenol a pH of 2.0 ± 0.2 was selected for both the activated carbons viz., SAC and ATSAC. Higher adsorption of phenols at lower pH has also been reported by others [37]. At the lower pH, the functional groups on the carbon surface are in the protonated form and high electron density on the solute molecules would lead to higher adsorption. In the acid range pH_{equ} increases with the increasing pH_{in}, i.e. neutralization and sorption process are parallel processes and after pH_{in} 8.0, the pH_{equ} decreases in all the cases (Fig. 4b). A similar trend has been reported for the adsorption of pyridine derivatives on the activated carbons [41]. The surface chemistry of the activated carbons essentially depends on their heteroatom content, mainly on their surface oxygen complex [42]. The surface charge would depend on the solution pH and the surface characteristics of the carbon. A negative charge will result from the dissociation of surface oxygen complexes of acid character such as carboxyl and phenolic groups and these surface sites are known to be Bronsted type. The positive surface charge may be due to surface oxygen complexes of basic character like pyrones or chromenes, or due to the existence of electron-rich regions within the graphene layers acting as Lewis basic centers, which accept protons from the aqueous solution [43].

The adsorption studies were carried out at 10, 25 and 40 °C to determine the adsorption isotherms. The isotherms for the adsorption of phenol and 2,4-dichlorophenol on the adsorbents developed from agricultural waste material viz., SAC and ATSAC at optimum pH and different temperatures are shown in Fig. 5a and b, respectively. The adsorption of both the adsorbates on the developed activated carbons increases with an increase in the temperature reflecting the endothermic nature of the reaction. Garcia-Araya et al. [37] and Mohan et al. [41] have also reported the endothermic processes for the adsorption of organic compounds on activated carbon. With the rise in the equilibrium concentrations (being more polar) the solute molecules interact via electrostatic interactions with the polar surface groups. This effect decreases with increase in the temperature enhancing the adsorption [44]. The isotherms are positive, regular and concave to the concentration axis (Fig. 5a and b). According to Giles' classification [45] the isotherms may be classified as H-type and L-type, for the adsorption of phenol and 2,4-dichlorophenol, respectively, on SAC, whereas, in case of ATSAC isotherms obtained for the adsorption of phenol were S-type and H-type for the adsorption of 2,4-dichlorophenol. The H-type isotherm indicates the high affinity of the activated carbon towards the adsorbate and that there is no strong competition from the solvent for sorption sites. The L-type isotherms suggest the completion of monolayer on the surface of adsorbent, while the S-type curve implies a side-by-side association between adsorbed molecules [45].

The Langmuir isotherms for the adsorption of phenol and 2,4-dichlorophenol on SAC and ATSAC at different temperatures are shown in Fig. 6a and b, respectively. The monolayer adsorption capacity (Q^0) was found to be higher for ATSAC as compared to SAC for adsorption of both phenol and 2,4-dichlorophenol (Table 2). The higher adsorption capacity (Q^0) for ATSAC, i.e.

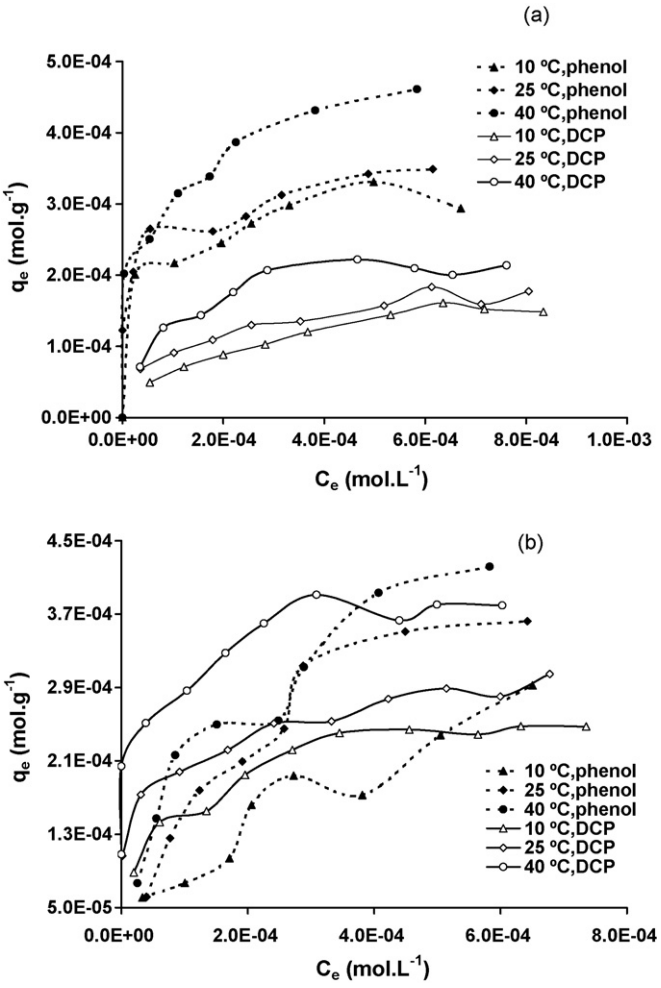

Fig. 5. Adsorption isotherms of phenol and 2,4-dichlorophenol on (a) SAC and (b) ATSAC at different temperatures and optimum pH.

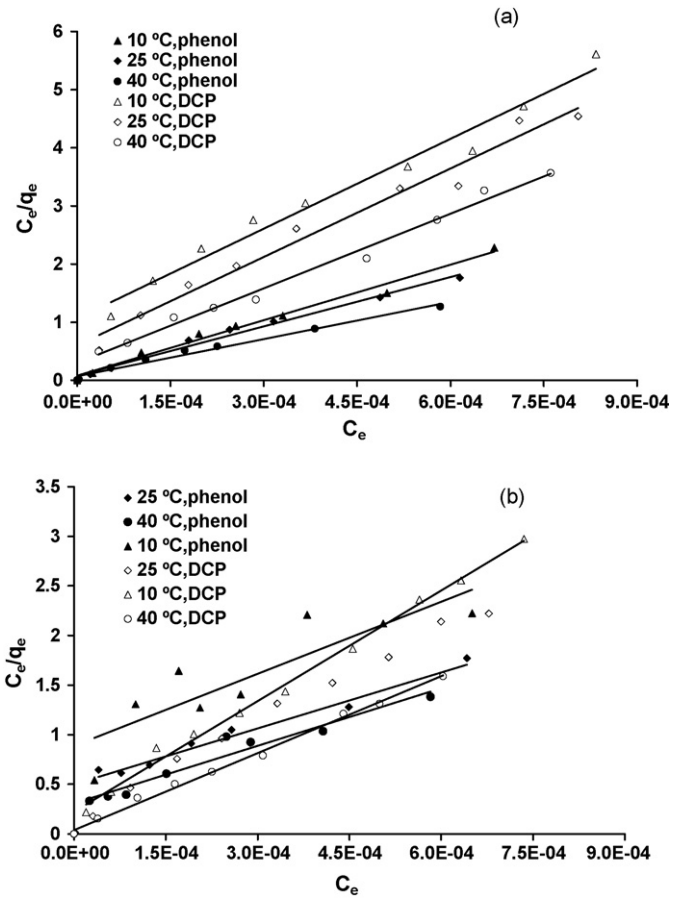

Fig. 6. Langmuir adsorption isotherms of phenol and 2,4-dichlorophenol on (a) SAC and (b) ATSAC at different temperatures and optimum pH.

the carbon prepared from the chemical treatment of the coconut shells may be due to its higher surface area than SAC. ATSAC has higher carbon content and pore volume, also, as compared to SAC. Similar conclusions have been drawn for the adsorption of pyridine and its derivatives on activated carbons [36,41]. The mechanism of phenol adsorption is determined by so-called "π–π interactions" and "donor–acceptor complex" formation. The first factor assumes that oxygen atoms bounded to the carbon reduce the π electron density and weaken the dispersion forces between phenol π electrons ring and the π electrons of carbons. The second one postulates that the adsorption mechanism is based on the formation of donor–acceptor complexes between the surface carbonyl groups (electron donors) and the aromatic rings of phenol acting as the acceptor [42,46,47]. Further, the sorption of phenol was higher than 2,4-dichlorophenol in case of both the developed adsorbents. This may be explained as the molecule of phenol is relatively smaller than 2,4-dichlorophenol molecule. Small molecules can access micropores driven by the strong adsorption potential near the micropore wall. The adsorption of phenol is mainly due to micropore filling [46]. The adsorption capacities of the developed adsorbents were compared with other adsorbents derived from different raw materials (Table 3). The adsorbents developed and used in this study have higher adsorption capacity for the adsorption of phenol as com-

Table 2
Langmuir isotherm constants for the adsorption

Adsorbent	10 °C			25 °C			40 °C		
	Q^0 ($\times 10^4$ mol g^{-1})	b ($\times 10^{-3}$ L mol^{-1})	R^2	Q^0 ($\times 10^4$ mol g^{-1})	b ($\times 10^{-3}$ L mol^{-1})	R^2	Q^0 ($\times 10^4$ mol g^{-1})	b ($\times 10^{-3}$ L mol^{-1})	R^2
Phenol									
SAC	3.22	28.14	0.99	3.63	24.63	0.99	4.85	21.46	0.99
ATSAC	4.13	2.73	0.76	5.32	3.76	0.96	5.17	6.28	0.95
2,4-Dichlorophenol									
SAC	1.94	4.86	0.98	1.97	8.46	0.98	2.34	14.32	0.99
ATSAC	2.69	16.52	0.99	3.07	24.94	0.99	3.99	35.11	0.99

Table 3
Adsorption capacities of various adsorbents for phenol

Adsorbent	Temperature (°C)	Q^0 (mmol g^{-1})	Reference
Bagasse fly ash	30	0.007	[1]
	40	0.006	
	50	0.005	
Carbonized bark			[31]
Data 1	23.26	0.35	
Data 2	23.26	0.43	
Oil-shale			[48]
KOH-OS	–	0.049	
$ZnCl_2$-OS	–	0.081	
Tamarind nut (TNSAC)	–	0.045	[49]
Date pits	25	0.185	[50]
Coconut shells			Present study
SAC	10	0.32	
	25	0.36	
	40	0.49	
ATSAC	10	0.41	
	25	0.53	
	40	0.52	

pared to those derived from bagasse fly ash, oil-shale, tamarind nut and date pits, whereas, it is comparable with that of the carbon developed from carbonized bark. The Langmuir constant '*b*' reflects the affinity of the adsorbent for the solute. For the adsorption of phenol the values of '*b*' are relatively higher for SAC indicating more stable bond/complex with carbon surface, while, for adsorption of 2,4-dichlorophenol ATSAC showed higher '*b*' values in comparison to SAC. The type (H-type) of isotherms for the adsorption of phenol on SAC (Fig. 5a) and 2,4-dichlorophenol (Fig. 5b) on ATSAC also suggests for the high affinity of the adsorbent. The essential characteristic of the Langmuir isotherm can be expressed in terms of a dimensionless equilibrium factor R_L that is defined as $R_L = 1/1 + bC_0$, where b is the Langmuir constant and C_0 is the initial concentration of adsorbate [51]. R_L values obtained (data not shown) at different concentrations and temperatures are between 0 and 1, indicating favourable adsorption of both adsorbates on activated carbons developed from the agricultural waste material.

The Freundlich isotherms for the adsorption of phenol and 2,4-dichlorophenol on SAC and ATSAC at different temperatures are presented in Fig. 7a and b, respectively. The linear plots of $\log q_e$ versus $\log C_e$ show that adsorption of phenol and 2,4-dichlorophenol on the SAC and ATSAC also follows the Freundlich isotherm model. The corresponding Freundlich

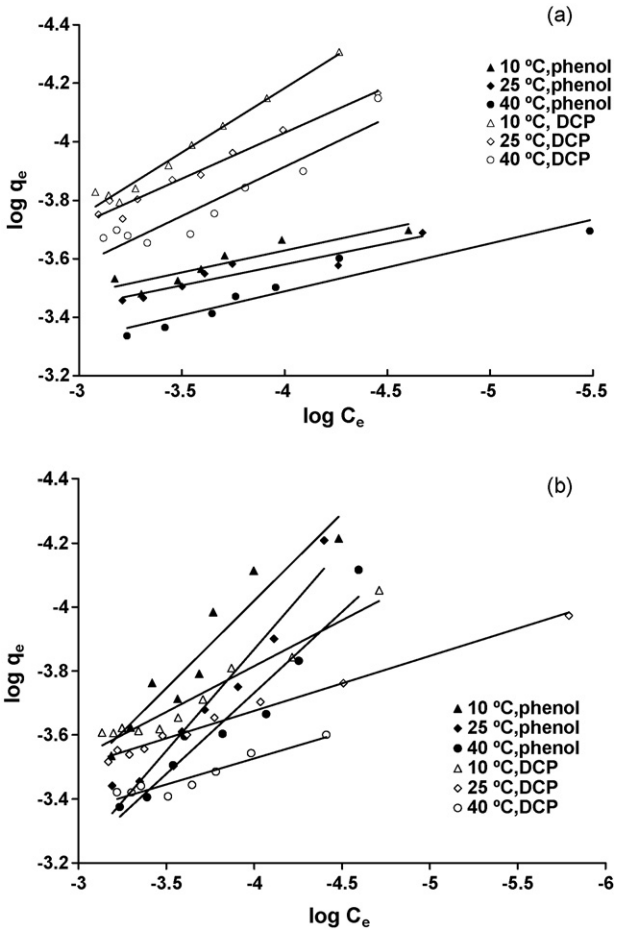

Fig. 7. Freundlich adsorption isotherms of phenol and 2,4-dichlorophenol on (a) SAC and (b) ATSAC at different temperatures and optimum pH.

isotherm parameters along with the correlation coefficients are given in Table 4. The value of $0 < 1/n < 1.0$ exhibits the favourability of adsorption onto activated carbons [52]. The correlation coefficients showed that in general, the Langmuir model fitted the results slightly better than the Freundlich model.

The thermodynamic parameters mainly free energy (ΔG°), enthalpy (ΔH°) and entropy (ΔS°) changes were calculated using Eqs. (6)–(8), respectively, to characterize the equilibrium of the system. The reference state was defined based on adsorption density in mol g^{-1} of adsorbent and concentration in mol L^{-1}:

$$\Delta G^\circ = -RT \ln k \quad (6)$$

Table 4
Freundlich isotherm constants for the adsorption

Adsorbent	10 °C			25 °C			40 °C		
	K_F ($\times 10^3$ mol g^{-1})	$1/n$	R^2	K_F ($\times 10^3$ mol g^{-1})	$1/n$	R^2	K_F ($\times 10^3$ mol g^{-1})	$1/n$	R^2
Phenol									
SAC	0.94	0.15	0.84	0.98	0.14	0.89	1.47	0.16	0.91
ATSAC	14.74	0.55	0.89	47.05	0.64	0.95	19.77	0.51	0.94
2,4-Dichlorophenol									
SAC	3.67	0.44	0.98	1.67	0.31	0.97	2.69	0.34	0.88
ATSAC	2.14	0.29	0.95	1.03	0.17	0.99	1.33	0.16	0.89

Table 5
Thermodynamic parameters of the adsorption

Adsorbent	$-\Delta G^\circ$ (kJ mol^{-1})			ΔH° (kJ mol^{-1})	ΔS° (kJ mol^{-1}K^{-1})
	10 °C	25 °C	40 °C		
Phenol					
SAC	24.10	25.05	25.96	−6.65	0.063
ATSAC	18.62	20.40	22.76	20.45	0.14
2,4-Dichlorophenol					
SAC	19.67	22.41	24.90	26.55	0.16
ATSAC	22.85	15.08	27.24	18.51	0.15

$$\Delta H^\circ = R\left(\frac{T_2 T_1}{T_2 - T_1}\right)\ln\frac{k_2}{k_1} \quad (7)$$

$$\Delta S^\circ = \frac{\Delta H^\circ - \Delta G^\circ}{T} \quad (8)$$

where k is the Langmuir constant same as b at different temperatures. The values obtained from thermodynamic analysis are given in Table 5. Positive values of ΔH° and ΔS° (for phenol-ATSAC, 2,4-dichlorophenol-SAC and 2,4-dichlorophenol-ATSAC) indicate the endothermic nature of the process. In case of phenol-SAC system negative value of ΔH° with positive ΔS° indicates that the process is favourable at all the temperatures [53]. The negative values of ΔG° for adsorption of phenol and 2,4-dichlorophenol indicate the feasibility and spontaneous nature of adsorption.

3.3. Kinetic studies

Concentration-time profiles for the adsorption of different adsorbates onto activated carbons at different experimental conditions are shown in Figs. 8 and 9. The extent of adsorption of both the adsorbates on SAC and ATSAC and their rate of removal are found to increase with temperature (Fig. 8a and b). The rate of removal of both the phenols increasing along with the increasing temperature indicates the endothermic nature of the process resembling with the results of thermodynamic analysis. The effect of adsorbent amount and initial adsorbate concentration on the removal of phenol at different carbons has also been studied. The rate of uptake increased with an increase in adsorbent amount (Fig. 1), whereas it increases with the increase in the initial concentration (Fig. 9a and b). The adsorption rate data for the studied adsorbates onto the developed activated carbons were analysed using two kinetic models viz., pseudo-first-order-

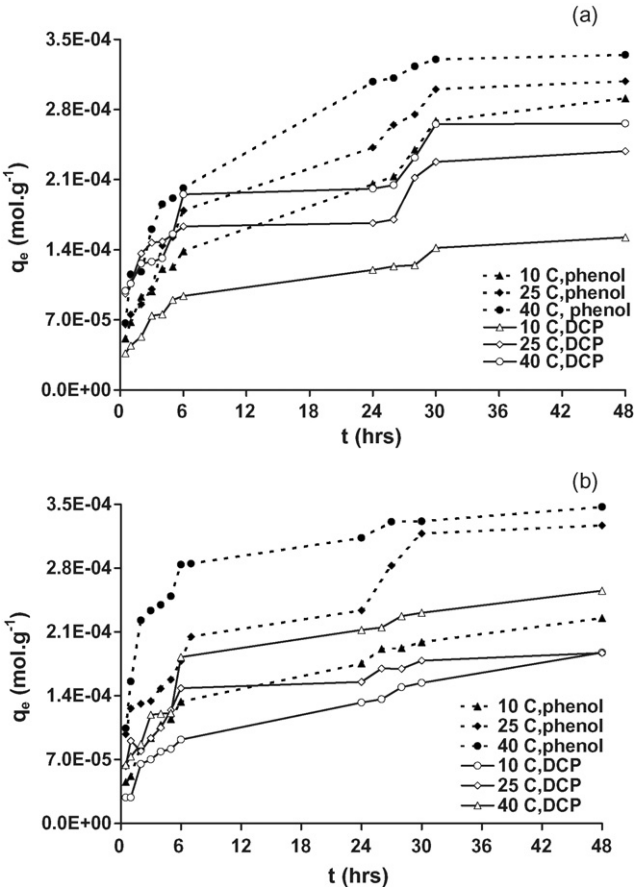

Fig. 8. Effect of temperature on the uptake of phenol and 2,4-dichlorophenol on (a) SAC and (b) ATSAC at optimum pH; adsorbent amount = 1.0 g L^{-1}; $C_0 = 5 \times 10^{-4}$ mol L^{-1}.

equation and pseudo-second-order-equation were tested. Both the models were studied at different temperatures to find out the effect of temperature on the rate-equation parameters. It was observed that the pseudo-first-order rate-constant (k_1) as well as the pseudo-second-order-rate-equation parameters (k_2, v_0 and q_e) generally increased with an increase in the temperature (Tables 6 and 7, respectively). The validity of the above two models was checked by studying the kinetics under different initial adsorbate concentrations as, in the case of first-order kinetic reaction, the half life time is independent from the initial adsorbate concentration. The adsorption parameters of first-order and second-order rate equations were calculated at three different initial concentrations of the each adsorbate viz., phenol and

Table 6
First-order rate constants for the adsorption at different temperatures

Adsorbent	10 °C		25 °C		40 °C	
	k_1 ($\times 10^3$ min^{-1})	R^2	k_1 ($\times 10^3$ min^{-1})	R^2	k_1 ($\times 10^3$ min^{-1})	R^2
Phenol						
SAC	0.94	0.87	1.36	0.86	1.86	0.95
ATSAC	0.95	0.97	1.27	0.79	1.29	0.90
2,4-Dichlorophenol						
SAC	0.94	0.88	0.83	0.65	1.51	0.92
ATSAC	0.74	0.96	1.16	0.89	1.04	0.94

Table 7
Second-order rate constants at different temperatures

Adsorbent	10 °C					25 °C					40 °C				
	V_0[a] ($\times 10^6$)	k_2[a]	q_e[a] ($\times 10^4$)	R^2	$t_{1/2}$	V_0 ($\times 10^6$)	k_2	q_e ($\times 10^4$)	R^2	$t_{1/2}$	V_0 ($\times 10^6$)	k_2	q_e ($\times 10^4$)	R^2	$t_{1/2}$
Phenol															
SAC	0.86	9.63	2.99	0.97	3.65	1.08	9.88	3.30	0.99	2.39	1.70	13.19	3.59	0.99	3.00
ATSAC	0.90	16.91	2.30	0.99	5.76	1.33	11.67	3.38	0.97	2.47	3.61	29.06	3.52	0.99	3.85
2,4-Dicholorophenol															
SAC	0.70	29.85	1.53	0.98	5.79	1.59	30.75	2.27	0.96	5.11	1.47	21.03	2.64	0.97	3.52
ATSAC	0.54	15.30	1.89	0.97	4.29	1.28	35.53	1.90	0.99	4.23	1.13	16.44	2.63	0.99	1.63

[a] $V_0 = (\text{mol g}^{-1}\ \text{min}^{-1})$, $k_2 = (\text{g mol}^{-1}\ \text{min}^{-1})$, $q_e = (\text{mol g}^{-1})$.

2,4-dichlorophenol using different studied carbons. The results obtained from both the first and second-order rate equations are summarized in Tables 8 and 9, respectively. Variation of half-life (t_{50}) with initial adsorbate (phenol and 2,4-dichlorophenol) concentration validates the adsorption reaction to be of the second-order rather than the first-order one. The q_e values were calculated using the pseudo-first-order and the second-order-rate equation and it was observed that the theoretical q_e values calculated using the second-order-rate equation agree more accurately with the experimental q_e values at different temperatures and initial adsorbate concentrations (Tables 10 and 11, respectively). These observations suggest that the studied sorption systems follow the second-order-rate equation instead of the first-order one. Mohan et al. [41] and Al-Asheh et al. [48] have also reported

Table 8
First-order rate constants for the adsorption at different initial adsorbate concentrations

Adsorbent	1×10^{-4} (mol L^{-1})		5×10^{-4} (mol L^{-1})		1×10^{-3} (mol L^{-1})	
	k_1 ($\times 10^3$ min^{-1})	R^2	k_1 ($\times 10^3$ min^{-1})	R^2	k_1 ($\times 10^3$ min^{-1})	R^2
Phenol						
SAC	1.85	0.66	1.36	0.86	1.14	0.88
ATSAC	7.17	0.93	1.27	0.79	1.06	0.92
2,4-Dichlorophenol						
SAC	0.84	0.83	0.83	0.65	1.06	0.62
ATSAC	1.41	0.94	1.16	0.89	1.32	0.97

Table 9
Second-order rate constants at different initial adsorbate concentrations

Adsorbent	$C_0 = 1 \times 10^{-4}$ (mol L^{-1})				$C_0 = 5 \times 10^{-4}$ (mol L^{-1})				$C_0 = 1 \times 10^{-3}$ (mol L^{-1})			
	V_0[a] ($\times 10^6$)	k_2[a]	q_e[a] ($\times 10^4$)	R^2	V_0 ($\times 10^6$)	k_2	q_e ($\times 10^4$)	R^2	V_0 ($\times 10^6$)	k_2	q_e ($\times 10^4$)	R^2
Phenol												
SAC	0.70	77.89	0.95	0.99	1.08	9.88	3.30	0.99	1.46	4.82	5.51	0.95
ATSAC	2.84	97.79	1.03	0.99	1.33	11.67	3.38	0.97	4.47	21.19	4.59	0.99
2,4-Dichlorophenol												
SAC	0.41	55.78	0.86	0.97	3.67	33.51	3.31	0.99	2.21	68.11	1.80	0.99
ATSAC	0.11	12.95	0.90	0.92	1.28	35.53	1.90	0.99	2.23	42.87	2.28	0.99

[a] $V_0 = (\text{mol g}^{-1}\ \text{min}^{-1})$, $k_2 = (\text{g mol}^{-1}\ \text{min}^{-1})$, $q_e = (\text{mol g}^{-1})$.

Table 10
Comparative evaluation of q_e as calculated experimentally and by using first and second-order rate equations at different temperatures

Adsorbent	$q_{e,exp}$ ($\times 10^4$ mol g^{-1})			$q_{e,cal\text{-}1}$ ($\times 10^4$ mol g^{-1})			$q_{e,cal\text{-}2}$ ($\times 10^4$ mol g^{-1})		
	10 °C	25 °C	40 °C	10 °C	25 °C	40 °C	10 °C	25 °C	40 °C
SAC	2.91	3.08	3.34	2.31	2.51	2.61	2.99	3.30	3.59
ATSAC	2.25	3.27	3.47	1.59	2.39	1.54	2.30	3.38	3.52
SAC	1.52	2.38	2.66	1.01	1.21	1.82	1.53	2.27	2.64
ATSAC	1.87	1.87	2.55	1.42	1.04	1.72	1.89	1.90	2.63

$q_{e,exp}$: experimental equilibrium concentration; $q_{e,cal\text{-}1}$: equilibrium concentration computed using first-order kinetic model; $q_{e,cal\text{-}2}$: equilibrium concentration computed using second-order kinetic model.

Table 11
Comparative evaluation of q_e as calculated experimentally and by using first and second-order rate equations at different initial adsorbate concentrations

Adsorbent	$q_{e,exp}$ ($\times 10^4$ mol g^{-1})			$q_{e,cal\text{-}1}$ ($\times 10^4$ mol g^{-1})			$q_{e,cal\text{-}2}$ ($\times 10^4$ mol g^{-1})		
	1×10^{-4} (mol L^{-1})	5×10^{-4} (mol L^{-1})	1×10^{-3} (mol L^{-1})	1×10^{-4} (mol L^{-1})	5×10^{-4} (mol L^{-1})	1×10^{-3} (mol L^{-1})	1×10^{-4} (mol L^{-1})	5×10^{-4} (mol L^{-1})	1×10^{-3} (mol L^{-1})
Phenol									
SAC	0.92	3.08	5.16	0.62	2.51	4.26	0.95	3.30	5.51
ATSAC	1.01	3.27	4.51	0.38	2.39	1.94	1.03	3.38	4.59
2,4-Dichlorophenol									
SAC	0.88	2.38	1.84	0.56	1.21	0.69	0.86	3.31	1.80
ATSAC	0.69	1.80	2.25	0.72	1.04	1.04	0.90	1.90	2.28

$q_{e,exp}$: experimental equilibrium concentration; $q_{e,cal\text{-}1}$: equilibrium concentration computed using first-order kinetic model; $q_{e,cal\text{-}2}$: equilibrium concentration computed using second-order kinetic model.

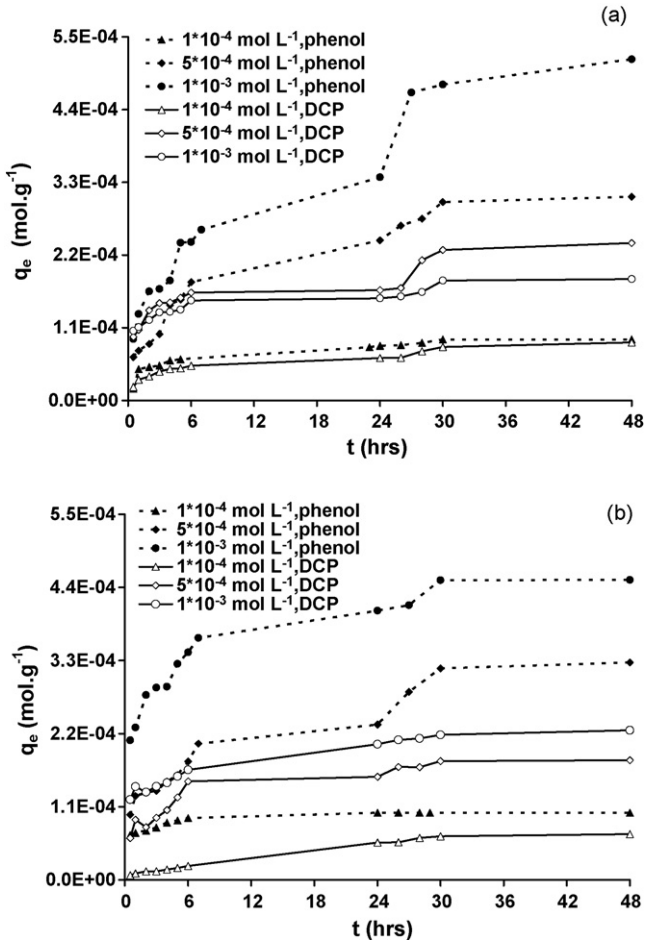

Fig. 9. Effect of initial adsorbate concentration on the uptake of phenol and 2,4-dichlorophenol on (a) SAC and (b) ATSAC at optimum pH; adsorbent amount = 1.0 g L^{-1}; temperature = 25 °C.

the pseudo-second-order rate equation for the adsorption of pyridine-derivative and phenol, respectively. Further, regression coefficients between experimental and calculated values obtained for the first-order rate model ($R^2 = 0.77$) and second-order rate equation ($R^2 = 0.97$) also indicate the suitability of the second-order-rate equation for the adsorption of both phenols on SAC and ATSAC.

The mass-transfer analysis of adsorbates during the process was studied by using the mass transfer diffusion model [54]:

$$\ln\left(\frac{C_t}{C_0} - \frac{1}{1+mk}\right) = \ln\left(\frac{mk}{mk}\right) - \left(\frac{1+mk}{mk}\right)\beta_L S_s t \qquad (9)$$

where C_t is the concentration of solute at time t (mol L^{-1}), C_0 the initial concentration of the solute (mol L^{-1}), m the mass of the adsorbent per unit volume of particle-free solution of solute (g L^{-1}), k the Langmuir constant (obtained by multiplying Q^0 with (b), β_L the mass transfer coefficient (cm s^{-1}) and S_s is the outer surface of the adsorbent per unit volume of particle-free slurry (cm^{-1}) and is calculated as:

$$S_s = \frac{6m}{(1-\varepsilon_p)d_p\rho_p} \qquad (10)$$

where d_p is the particle diameter (cm), ρ_p the density of adsorbent (g cm^{-1}) and ε_p is the porosity of adsorbent particles.

The values of β_L were determined from the slope and intercepts of the plots of $\ln\{(C_t/C_0) - (1/[(1+mk)]\}$ versus 't', for different temperatures and initial adsorbate concentrations (Figs. 10 and 11, respectively) using the least squares method. The linearity of the plots confirms the validity of the diffusion model for the studied adsorbate-adsorbent systems. The values of the mass transfer coefficient (β_L) of the adsorbates for both the developed adsorbents (SAC and ATSAC) are presented in Table 12. The values of β_L increased with an increase in the temperature, suggesting endothermic nature of the reaction. Further, it was found that increasing the initial adsorbate concentration results in a decrease in the external mass transfer coefficient. These findings are similar to those reported for the adsorption of phenol by coconut-husk based activated carbon [18].

To interpret the experimental data, it is necessary to identify the rate-determining step controlling the removal rate in the adsorption process. The three consecutive steps involved in the adsorption of an organic/inorganic species by a porous adsorbent are:

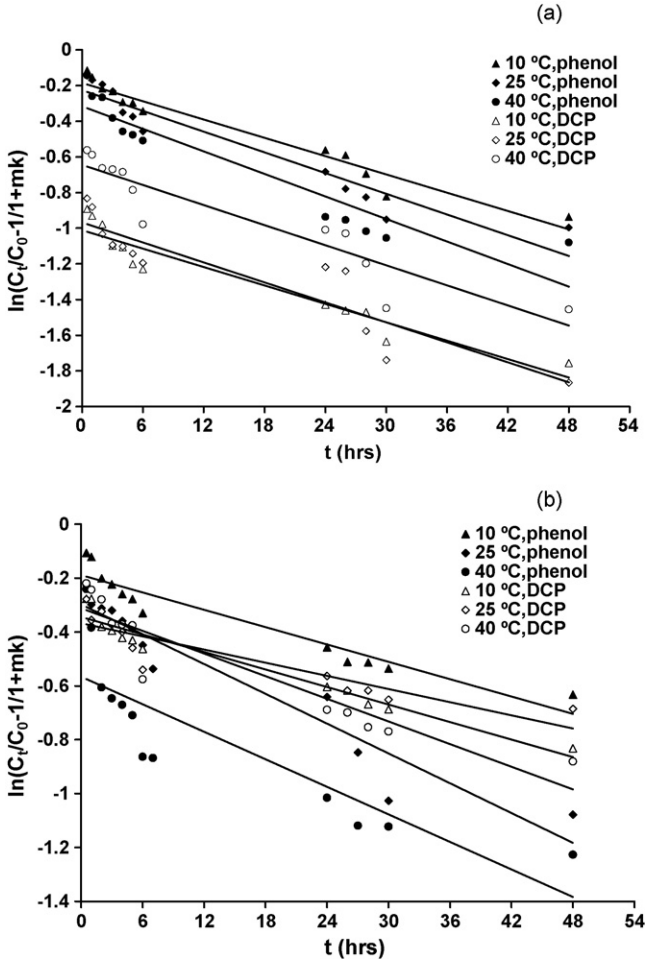

Fig. 10. McKay plots for the adsorption of phenol and 2,4-dichlorophenol on (a) SAC and (b) ATSAC at different temperatures (optimum pH; $C_0 = 5 \times 10^{-4}$ mol L^{-1}).

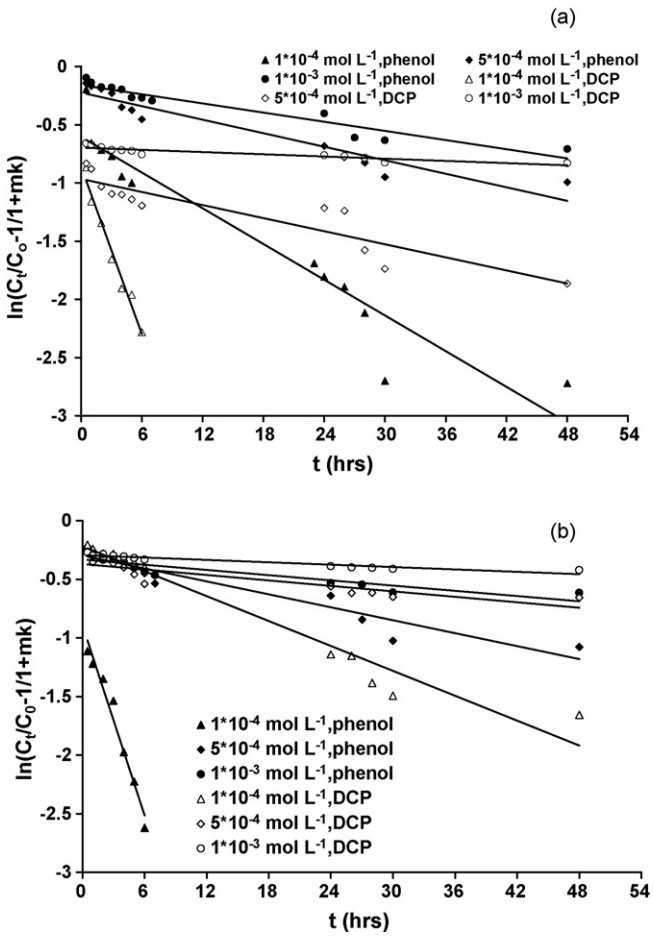

Fig. 11. McKay plots for the adsorption of phenol and 2,4-dichlorophenol on (a) SAC and (b) ATSAC at different initial concentrations (optimum pH; temperature = 25 °C).

(1) transport of the adsorbate to the external surface of the adsorbent (film-diffusion);
(2) transport of the adsorbate within the pores of the adsorbent except for a small amount of adsorption that occurs on the external surface (particle diffusion);
(3) adsorption of the adsorbate on the external surface of the adsorbent.

It is, generally, accepted that the process (3) is very rapid and does not represent the rate-determining step in the uptake of organic/inorganic species. For the remaining two steps in the overall transport three distinct cases occur: (i) external transport > internal transport; (ii) external transport < internal transport; and (iii) external transport ≈ internal transport. In case (i) and (ii) the rate is governed by film and particle diffusion, respectively. In case (iii), the transport of ions to the boundary may not be possible at a significant rate, leading to the formation of a liquid film with a concentration gradient surrounding sorbent particles. Usually, external transport is the rate limiting step in systems having (a) poor mixing; (b) dilute concentration of adsorbate; (c) small particle size; and (d) high affinity of adsorbent, whereas, intra-particle step limits the overall transfer for the systems which have (a) high concentration of adsorbate;

Table 12
Mass transfer coefficients (β_L) at different temperatures and initial adsorbate concentrations

Adsorbent	Temperature						Initial concentrations					
	10 °C		25 °C		40 °C		1×10^{-4} (mol L^{-1})		5×10^{-4} (mol L^{-1})		1×10^{-3} (mol L^{-1})	
	β_L ($\times 10^7$ cm s^{-1})	R^2	β_L ($\times 10^7$ cm s^{-1})	R^2	β_L ($\times 10^7$ cm s^{-1})	R^2	β_L ($\times 10^7$ cm s^{-1})	R^2	β_L ($\times 10^7$ cm s^{-1})	R^2	β_L ($\times 10^7$ cm s^{-1})	R^2
Phenol												
SAC	3.86	0.95	4.36	0.92	5.27	0.88	11.49	0.91	4.36	0.92	2.94	0.92
ATSAC	1.17	0.91	2.53	0.92	2.68	0.74	37.39	0.97	2.53	0.92	1.01	0.81
2,4-Dichlorophenol												
SAC	2.08	0.91	2.92	0.83	3.62	0.86	37.46	0.97	2.92	0.83	0.5	0.82
ATSAC	1.47	0.94	1.82	0.82	2.69	0.88	6.46	0.96	1.47	0.79	0.62	0.90

(b) good mixing; (c) large particle size of adsorbent; and (d) low affinity of adsorbent for adsorbate. The kinetic studies data were analyzed by the procedure given by Reichenberg [55] and Helffrich [56] using following equations:

$$F = 1 - \frac{6}{\pi^2}\sum_{n=1}^{\infty}\frac{1}{n^2}\exp\left[\frac{-D_i t\pi^2 n^2}{r_0^2}\right] \quad (11)$$

or

$$F = 1 - \frac{6}{\pi^2}\sum_{n=1}^{\infty}\frac{1}{n^2}\exp[-n^2 B_t] \quad (12)$$

where F is the fractional attainment of equilibrium at time 't' and is obtained by the expression:

$$F = \frac{Q_t}{Q^0} \quad (13)$$

where Q_t is the amount of adsorbate taken up at time 't' and Q^0 is the maximum equilibrium uptake and:

$$B = \frac{\pi^2 D_i}{r_0^2} \quad (14)$$

where D_i is the effective diffusion coefficient of adsorbate in the adsorbent phase, r_0 the radius of the adsorbent particle, assumed to be spherical, and 'n' is an integer that defines the infinite series solution.

B_t values were obtained for each observed value of F, from Reichenberg's table [55] and the results are plotted in Fig. 12a and b. The linearity test of B_t versus t plots was employed to distinguish between the film diffusion and particle diffusion controlled adsorption. If the plots of B_t versus 't' (having slope B) is a straight line passing through the origin, then the adsorption rate is governed by particle diffusion mechanism, otherwise it is governed by film diffusion. In case of SAC the B_t versus 't' plot for adsorption of phenol, at lower concentrations ($<1 \times 10^{-3}$ mol L^{-1}) and for 2,4-dichlorophenol (at initial concentration $> 1 \times 10^{-4}$ mol L^{-1}) do not pass through the origin, suggesting that the rate controlling process may be the film diffusion. In case of ATSAC, B_t versus t plots for phenol (at all the studied concentrations) and 2,4-dichlorophenol (at higher concentrations ($>5 \times 10^{-4}$ mol L^{-1}) do not pass through the origin. This suggests that here also the film diffusion process may be the rate-controlling step. However, in all the cases the B_t versus "t" plots (curved at later stage) can be resolved into two plots with different slopes, indicating change in the adsorption mechanism with time. It has also been suggested that change in the slope indicate the existence of different sizes of pores [57]. Similar types of observations have been reported for sorption of phenol [48] and metals [58]. In our study, the later portion of the curves, the slope increases and consequently the diffusion coefficient (D_i) increases. At this stage, in addition to film-diffusion other factors such as aggregation and electrokinetic interactions may also contribute [58]. The effective diffusion coefficients (D_i), for the adsorption on both the adsorbents (SAC and ATSAC) estimated from the slops of the B_t versus t plots (for the initial portion) decreases with an increase in the initial concentration

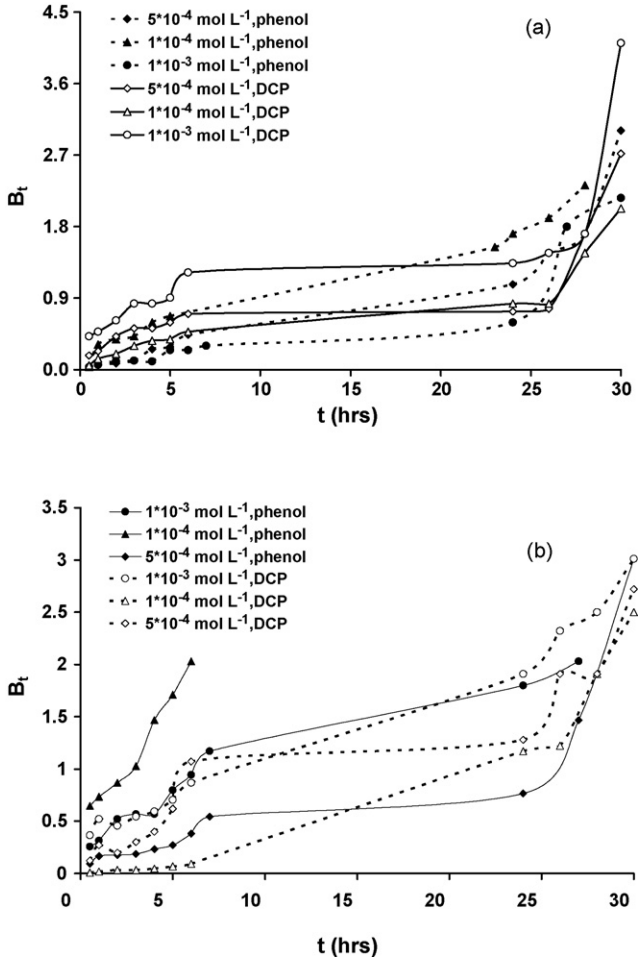

Fig. 12. B_t vs. t plots for the adsorption of phenol and 2,4-dichlorophenol on (a) SAC and (b) ATSAC at different initial concentrations (optimum pH; temperature = 25 °C).

of the phenol. However, the values of D_i were found to increase with the increasing initial concentration of 2,4-dichlorophenol (Table 13). Increase in the D_i values with increasing initial concentration may be explained as increasing solute concentration in the solution may reduce the diffusion of solute in the boundary layer and may enhance the diffusion in the solid as have been reported for the adsorption of the phenol onto activated carbon [17,18]. The effective diffusion coefficients (D_i) were also estimated at different temperatures (plots omitted for brevity) and are given in Table 13. Diffusion coefficient values for the SAC-adsorbate system at different temperatures were observed to decrease with an increase in temperature, while, the values of diffusion coefficient for ATSAC-adsorbate system were found to increase with an increase in temperature. Mohan et al. [41] have also reported similar trend of D_i values with the change in temperature for the adsorption of pyridine derivatives onto activated carbon, suggesting that the increased mobility of adsorbate molecules and a decrease in retarding forces acting on the diffusing adsorbate molecules results in the increase of D_i values with temperature.

The energy of activation (E_a), entropy of activation ($\Delta S^{\#}$) and pre-exponential factor (D_0) analogous to the Arrhenius

Table 13
Diffusion coefficients (D_i) at different temperatures and initial adsorbate concentrations

Adsorbent	Temperature						Initial concentrations					
	10 °C		25 °C		40 °C		1×10^{-4} (mol L^{-1})		5×10^{-4} (mol L^{-1})		1×10^{-3} (mol L^{-1})	
	D_i ($\times 10^{14}$ m^2 s^{-1})	R^2	D_i ($\times 10^{14}$ m^2 s^{-1})	R^2	D_i ($\times 10^{14}$ m^2 s^{-1})	R^2	D_i ($\times 10^{14}$ m^2 s^{-1})	R^2	D_i ($\times 10^{14}$ m^2 s^{-1})	R^2	D_i ($\times 10^{14}$ m^2 s^{-1})	R^2
Phenol												
SAC	2.84	0.93	1.84	0.85	1.21	0.83	1.51	0.93	1.14	0.97	0.60	0.92
ATSAC	1.27	0.98	1.75	0.76	1.84	0.92	6.56	0.97	1.75	0.76	1.58	0.93
2,4-Dichlorophenol												
SAC	1.29	0.88	1.23	0.62	0.97	0.83	1.86	0.97	2.31	0.94	3.38	0.94
ATSAC	0.93	0.97	1.44	0.89	1.73	0.95	1.32	0.97	1.62	0.73	1.66	0.99

Table 14
Thermodynamic parameters of activation

Adsorbent	D_0 ($m^2\,s^{-1}$)	E_a ($kJ\,mol^{-1}$)	$-\Delta S^{\#}$ ($J\,K^{-1}\,mol^{-1}$)
Phenol			
SAC	3.9×10^{-18}	20.96	230.45
ATSAC	6.6×10^{-13}	9.21	130.26
2,4-Dichlorophenol			
SAC	6.8×10^{-16}	7.01	187.41
ATSAC	1.2×10^{-12}	11.06	125.53

frequency factor were also determined (Table 14) using the following equations:

$$D_i = D_0 \exp\left[-\frac{E_a}{RT}\right] \quad (15)$$

$$D_0 = 2.72 d^2 \frac{kT}{h} \exp\left[\frac{\Delta S^{\#}}{R}\right] \quad (16)$$

where k is the Boltzman constant, h = Planck constant, R = gas constant, and d is the distance between two active sites of the adsorbent which is conventionally taken as 5 Å in inorganic ion exchangers, minerals and other adsorbents similar to carbon. The negative $\Delta S^{\#}$ values for the adsorption of phenol on activated carbons indicate that no significant changes occur in the internal structure of adsorbent material using adsorption.

4. Conclusions

Activated carbons developed from the coconut shells were characterized for various physical/chemical properties and studied for the adsorption of phenol and 2,4-dichlorophenol under different conditions. Adsorption of both the phenols increased with an increase in temperature. Both the Freundlich and Langmuir isotherm models adequately fit to the adsorption data. The pseudo-second-order-rate model better explained the adsorption kinetics as compared to the pseudo-first-order-rate model. The adsorption capacity (at 25 °C) of SAC and ATSAC for phenol was 0.36 and 0.53 mmol g^{-1}, respectively. In case of 2,4-DCP the adsorption capacity of SAC and ATSAC was about 0.20 and 0.31 mmol g^{-1}, respectively. The adsorbent developed after the chemical treatment (ATSAC) exhibited relatively higher monolayer adsorption capacity for the phenol and 2,4-dichlorophenol as compared to the one developed with thermal activation (SAC). Results of mass transfer analysis suggested the endothermic nature of the reaction and change in the mechanism with time and initial concentration of the adsorbate. The adsorption capacities of developed adsorbents are higher than those derived from other waste materials such as bagasse fly ash, oil-shale, tamarind nut and date pits. The results of this study show that the activated carbons derived from coconut shells can be used as potential adsorbent for phenols in water/wastewater.

Acknowledgements

The authors thank the Director, Industrial Toxicology Research Centre, Lucknow for providing the necessary facilities and his keen interest in this work. The authors are also thankful to Professor Vicente Gomez Serrano, Universidad Extremadura, Spain for carrying out the characterization of the prepared adsorbents.

References

[1] V.K. Gupta, S. Sharma, I.S. Yadav, D. Mohan, Utilization of bagasse fly ash generated in the sugar industry for the removal and recovery of phenol and *p*-nitrophenol from wastewater, J. Chem. Technol. Biotechnol. 71 (1998) 180–186.
[2] R. Spandre, G. Dellomonaco, Polyphenol pollution by olive mill waste waters, Tuscany, Italy, J. Environ. Hydrol. 4 (1996) 1–13.
[3] ATSDR (Agency for Toxic Substances and Disease Registry), Toxicological Profile for Phenol, US Department of Health and Human Services, USA, 1998.
[4] USEPA, Technical Support Document for Water Quality Based Toxics Control. EPA/440/485032, United States Environmental Protection Agency, Washington, DC, USA, 1985.
[5] BIS, Tolerance Limit for Industrial Effluents Discharged into Inland Surface Waters: Coke Oven. IS 2490 (Part 1), Bureau of Indian Standards, New Delhi, 1974.
[6] C. Barbeau, L. Deschenes, D. Karamanev, Y. Comeau, R. Samson, Bioremediation of pentachlorophenol contaminated soil by bio-augmentation using activated soil, Appl. Microbiol. Biotechnol. 48 (1997) 745–752.
[7] E. Leyva, E. Moctezuma, M.G. Ruiz, L. Torresmartinez, Photo-degradation of phenol and 4-chlorophenol by $BaO–Li_2O–TiO_2$ catalysts, Catal. Today 40 (1998) 367–376.
[8] A. Agrios, K. Gray, E. Weitz, Photocatalytic transformation of 2,4,5-trichlorophenol on TiO_2 under sub-band-gap illumination, Langmuir 19 (2003) 1402–1409.
[9] I.Z. Shirgaonkar, A.B. Pandit, Sonophotochemical destruction of aqueous solution of 2,4,6-trichlorophenol, Ultrason. Sonochem. 5 (1998) 53–61.
[10] A.B. Pandit, P.R. Gogate, S. Mujumdar, Ultrasonic degradation of 2:4:6 trichlorophenol in presence of TiO_2 catalyst, Ultrason. Sonochem. 8 (2001) 227–231.
[11] I.D. Buchanan, J.A. Micell, Peroxidase catalyzed removal of aqueous phenol, Biotechnol. Bioeng. 54 (1997) 251–261.
[12] M.C. Burleigh, M.A. Markowitz, M.S. Spector, B.P. Gaber, Porous polysilsesquioxanes for the adsorption of phenols, Environ. Sci. Technol. 36 (2002) 2515–2518.
[13] K.P. Singh, D. Mohan, S. Sinha, G.S. Tandon, D. Ghosh, Colour removal from wastewater using low cost activated carbon derived from agricultural waste material, Ind. Eng. Chem. Res. 42 (2003) 1965–1976.
[14] N.A. Darwish, K.A. Halhouli, N.M. Al-Dhoon, Adsorption of phenol from aqueous systems onto oil shale, Sep. Sci. Technol. 31 (1996) 705–714.
[15] K. Srinivasan, P.B.S. Rao, A. Ramadevi, Studies on characteristics of carbon obtained from tamarind nut, Ind. J. Environ. Hlth. 30 (1998) 303–311.
[16] C. Flock, A. Bassi, M. Gijzen, Removal of aqueous phenol and 2-chlorophenol with purified soybean peroxidase and raw soybean hulls, J. Chem. Technol. Biotechnol. 74 (1999) 303–309.
[17] N.B. Sankaran, T.S. Anirudhan, Adsorption dynamics of phenol on activated carbon produced from Salvinia molta Mitchell by single-step steam pyrolysis, Indian J. Eng. Mater. Sci. 6 (1999) 229–238.
[18] V.P. Vinod, T.S. Anirudhan, Effect of experimental variables on phenol adsorption on activated carbon prepared from coconut husk by single-step steam pyrolysis: mass transfer process and equilibrium studies, J. Sci. Ind. Res. 61 (2002) 128–138.
[19] Al. Vogel, A Text Book of Quantitative Chemical Analysis, ELBS Publication, London, England, 1991.
[20] G. McKay, Use of Adsorbents for the Removal of Pollutants from Wastewater, CRC Press, Boca Raton, FL, 1995.
[21] W.J. Weber Jr., Physico-chemical Processes for Water Quality Control, Wiley–Interscience, New York, 1972.
[22] D. Mohan, K.P. Singh, Single- and multi-component adsorption of cadmium and zinc using activated carbon derived from bagasse-an agricultural waste, Water Res. 36 (2002) 2304–2318.

[23] K. Laszlo, E. Tombacz, P. Kerepesi, Surface chemistry of nanoporous carbon and the effect of pH on adsorption from aqueous phenol and 2,3,4-trichlorophenol solutions, Colloid Surf. A: Physicochem. Eng. Aspects 13 (2004) 230–238.
[24] E. Tutem, R. Apak, G.F. Unal, Adsorptive removal of chlorophenols from water by bituminous shale, Water Res. 32 (1998) 2315–2324.
[25] Z. Reddad, C. Gerente, Y. Andres, P.L. Cloirec, Adsorption of several metal ions onto a low-cost biosorbent: kinetic and equilibrium studies, Environ. Sci. Technol. 36 (2002) 2067–2073.
[26] C. Ishizaki, I. Marti, Surface oxide structures on a commercial activated carbon, Carbon 19 (1981) 409.
[27] V.A. Garten, D.E. Weiss, A new interpretation of the acidic and basic structures in carbons, Aust. J. Chem. 10 (1957) 295–308.
[28] C. Selomulya, V. Meeyoo, R. Amal, Mechanisms of Cr(VI) removal from water by various types of activated carbons, J. Chem. Technol. Biotechnol. 74 (1999) 111–122.
[29] F. Rodriguez-Reinoso, Activated carbon: structure characterization preparation and applications, in: H. Marsh, E.A. Heintz, F. Rodriguez-Reinoso (Eds.), Introduction to Carbon Technologies, Chapter, 1997.
[30] A. Dabrowski, P. Podkoscielny, Z. Hubicki, M. Barczak, Adsorption of phenolic compounds by activated carbon—a critical review, Chemosphere 58 (2005) 1049–1070.
[31] R.U. Edgehill, G.Q. Lu, Adsorption characteristics of carbonized bark for phenol and pentachlorophenol, J. Chem. Technol. Biotechol. 71 (1998) 27–34.
[32] P. Podkoscielny, A. Dabrowski, O.V. Marijuk, Heterogeneity of active carbons in adsorption of phenol aqueous solutions, Appl. Surf. Sci. 205 (2003) 297–303.
[33] D.M. Nevskaia, A. Santianes, V. Munoz, A. Guerrero-Ruiz, Interaction of aqueous solutions of phenol with commercial activated carbons: an adsorption and kinetic study, Carbon 37 (1999) 1065–1074.
[34] R. Quadeer, A.H. Rehan, A study of the adsorption of phenol by activated carbon from aqueous solutions, Turk. J. Chem. 26 (2002) 357–361.
[35] A. Bembnowska, R. Pelech, E. Milchert, Adsorption from aqueous solutions of chlorinated organic compounds onto activated carbons, J. Colloid Interf. Sci. 265 (2003) 276–282.
[36] D. Mohan, K.P. Singh, S. Sinha, D. Ghosh, Removal of pyridine from aqueous solution using low-cost activated carbons derived from agricultural waste material, Carbon 42 (2004) 2409–2421.
[37] J.F. Garcia-Araya, F.J. Beltran, P. Alvarez, F.J. Masa, Activated carbon adsorption of some phenolic compounds present in agroindustrial wastewater, Adsorption 9 (2003) 107–115.
[38] F.A. Banat, B. Al-Bashir, S. Al-Asheh, O. Hayajneh, Adsorption of phenol by bentonite, Environ. Pollut. 107 (2000) 391–398.
[39] N. Khalid, S. Ahmad, A. Toheed, J. Ahmad, Potential of rice husk for antimony removal, Appl. Radiat. Isotopes 52 (2000) 30–38.
[40] S. Nouri, F. Haghseresht, Adsorption of *p*-nitrophenol in untreated and treated activated carbon, Adsorption 10 (2004) 79–86.
[41] D. Mohan, K.P. Singh, S. Sinha, D. Ghosh, Removal of pyridine derivatives from aqueous solution using low-cost activated carbons derived from agricultural waste material, Carbon 43 (2005) 1680–1693.
[42] L.R. Radovic, C. Moreno-Castilla, J. Rivera-Utrilla, Carbon materials as adsorbents in aqueous solutions, in: L.R. Radovic (Ed.), Chemistry and physics of Carbon, vol. 27, Marcel Dekker, New York, 2001.
[43] C. Moreno-Castilla, Adsorption of organic molecules from aqueous solutions on carbon materials, Carbon 42 (2004) 83–94.
[44] A.P. Terzyk, Further insights into the role of carbon surface functionalities in the mechanism of phenol adsorption, J. Colloid Interf. Sci. 268 (2003) 301–329.
[45] C.H. Giles, T.H. MacEwan, S.N. Nakhwa, D.C. Smith, Studies in adsorption. Part XI. A system of classification of solution adsorption isotherms, and its use in diagnosis of adsorption mechanisms and in measurement of specific surface areas of solids, J. Chem. Soc. 3 (1960) 3973–3993.
[46] F. Su, L. Lv, T.M. Hui, X.S. Zhao, Phenol adsorption on zeolite-templated carbons with different structural and surface properties, Carbon 43 (2005) 1156–1164.
[47] J.S. Mattson, H.B. Mark Jr., M.D. Malbin, W.J. Weber Jr., J.C. Crittenden, Surface chemistry of active carbon: specific adsorption of phenols, J. Colloid Interf. Sci. 31 (1969) 116–130.
[48] S. Al-Asheh, F. Banat, A. Masad, Physical and chemical activation of pyrolyzed oil shale residue for the adsorption of phenol from aqueous solutions, Environ. Geol. 44 (2003) 333–342.
[49] V.V. Goud, K. Mohanty, M.S. Rao, N.S. Jayakumar, Phenol removal from aqueous solutions by tamarind nutshell activated carbon: batch and column studies, Chem. Eng. Technol. 28 (2005) 814–821.
[50] M.A. Abdulkarim, N.A. Darwish, Y.M. Magdy, A. Dwaidar, Adsorption of phenolic compounds and methylene blue onto activated carbon prepared from date fruit pits, Eng. Life Sci. 2 (2002) 161–165.
[51] T.W. Weber, R.K. Chakravorti, Pore and solid diffusion models for fixed-bed adsorbers, J. Am. Inst. Chem. Eng. 20 (1974) 228–238.
[52] G. McKay, H.S. Blair, J.R. Garden, Adsorption of dyes on chitin. I. Equilibrium studies, J. Appl. Poly. Sci. 27 (1982) 3043–3057.
[53] J.C. Kuriacose, J. Rajaram, Chemistry in engineering and technology General and Physical Chemistry, vol. 1, Tata McGraw-Hill, New Delhi, India, 1984.
[54] G. McKay, M.S. Otterburn, A.G. Sweeney, Surface mass transfer process during colour removal from effluent using silica, Water Res. 15 (1981) 327–331.
[55] D. Reichenberg, Properties of ion-exchange resin in relation to their structure. III. Kinetics of exchange, J. Am. Chem. Soc. 75 (1953) 589–597.
[56] F. Helffrich, Ion-exchange, McGraw-Hill, New York, 1962.
[57] S.M. Hasany, M.M. Saeed, M. Ahmad, Adsorption isotherms and thermodynamic profile of Co(II)SCN complex uptake on polyurethane foam, Sep. Sci. Technol. 35 (2000) 379–394.
[58] V.K. Gupta, S. Sharma, Removal of cadmium and zinc from aqueous solutions using red mud, Environ. Sci. Technol. 36 (2002) 3612–3617.